International Journal for Uncertainty Quantification, 2 (2): 95–110 (2012)

ROBUST STOCHASTIC DESIGN OF BASE-ISOLATED STRUCTURAL SYSTEMS

Hector Jensen, [*] ***Juan Sepulveda, & Luis Becerra***

Departmento de Obras Civiles, Universidad Tecnica Federico Santa Maria, Valparaiso, Chile

Original Manuscript Submitted: 5/4/2011; Final Draft Received: 8/9/2011

The development of a general framework for robust reliability-based design of base-isolated structural systems under uncertain conditions is presented. The uncertainties about the structural parameters as well as the variability of future excitations are characterized in a probabilistic manner. Isolation elements composed of nonlinear lead rubber bearings are used to model the isolation system. The optimal design problem is formulated as a nonlinear constrained minimization problem involving multiple design requirements, including reliability constraints related to the structural performance. Failure events defined by a large number of random variables are used to characterize the reliability of the system. A sequential optimization approach based on global conservative, convex, and separable approximations is implemented for solving the optimization problem. An example problem that considers a 10-story building under stochastic ground excitation illustrates the beneficial effects of base-isolation systems in reducing the superstructure response.

KEY WORDS: *approximation strategies, base-isolated structural systems, common random numbers, nonlinear optimization, robust reliability, sensitivity analysis, simulation methods, stochastic optimization*

1. INTRODUCTION

There has been growing interest in recent years in the application of base-isolation techniques in order to improve the earthquake resistant performance of civil structures such as buildings, bridges, nuclear reactors, etc. [1–4]. In fact, the potential advantages of seismic isolation and the recent advancements in isolation-system products have led to the design and construction of an increasing number of seismically isolated structural systems. Also, seismic isolation is extensively used for seismic retrofitting of existing structures [5, 6]. One of the difficulties in the design of base-isolated structural systems is the explicit consideration of the nonlinear behavior of the isolators during the design process. Similarly, the consideration of uncertainty about the structural model and the potential variability of future ground motions are major challenges in the analysis and design of these systems. In view of these issues, this work introduces a general framework for robust reliability-based design of base-isolated structural systems under uncertain conditions. The uncertainty about the structural and excitation model parameters is characterized in a probabilistic manner. A probability density function that incorporates available knowledge about the system is assigned to the uncertain parameters involved in the problem. In this setting the design process is called robust stochastic system design and the associated design optimization problem, stochastic design optimization. The uncertain ground excitation is modeled as a nonstationary stochastic process with uncertain model parameters. In particular, a class of point-source models is adopted in the present formulation [7]. It is emphasized that the purpose of this contribution is not in the development of a specific stochastic model for ground motions but to introduce a general framework for solving a challenging class of structural optimization problems. Isolation elements composed by uniaxial lead rubber bearings are used to model the isolation system. The hysteretic behavior of the bearings is characterized by the Bouc-Wen-type model [8]. The reliability-based design is formulated as a nonlinear constrained minimization problem involving multiple design requirements, including reliability constraints. First excursion probabilities that account for the uncertainty

[*]Correspond to Hector Jensen, E-mail: hector.jensen@usm.cl

2152–5080/12/$35.00

in the system parameters as well as in the excitation are used to characterize the system reliability. Such probabilities are estimated by an adaptive Markov chain Monte Carlo procedure [9]. A sequential optimization approach based on global conservative, convex, and separable approximations is implemented for solving the optimization problem [10–12]. The optimization scheme is combined with the use of common random numbers throughout all iterations in the optimization process. The approach explicitly takes into account all nonlinear characteristics of the combined structural system (superstructure-isolation system) during the design process. A numerical example is presented to illustrate the applicability and effectiveness of the proposed framework in the context of reliability-based optimal design of base-isolated systems in the presence of uncertainties.

2. STOCHASTIC DESIGN PROBLEM

The stochastic design problem is defined as the identification of a vector $\{\phi\}$ of design variables that minimizes an objective function, that is

$$\text{Minimize } f(\{\phi\}) \tag{1}$$

subject to design constraints

$$h_j(\{\phi\}) \leq 0 \ \ , \ \ j = 1, ..., n_c \tag{2}$$

and side constraints

$$\{\phi\} \in \Phi \tag{3}$$

where $\Phi \in R^{n_d}$ denotes the admissible design space. The objective function is defined in terms of quantities such as initial, construction, repair, or downtime costs. On the other hand, the design constraints are given in terms of reliability constraints and/or constrains related to deterministic design requirements. The concept of robust reliability is used in the present formulation to quantify the stochastic performance of the system under design. The reliability constraints are defined in terms of failure probabilities. In particular, the probability that design requirements are satisfied within a particular reference period is used as the reliability measure. Such a measure is referred to as the first excursion probability and provides a measure of the plausibility of the occurrence of unacceptable behavior of the system (failure), based on the available information. The probability of failure $P_{F_j}(\{\phi\})$ corresponding to a failure event F_j evaluated at the design $\{\phi\}$ can be expressed in terms of the multidimensional probability integral [13, 14]

$$P_{F_j}(\{\phi\}) = \int_{\Theta} I_{F_j}(\{\phi\}, \{\theta\})\, q(\{\theta\}|\{\phi\})\, d\{\theta\} \tag{4}$$

where $I_{F_j}(\{\phi\}, \{\theta\})$ is the indicator function for failure, which is equal to 1 if the system fails and zero otherwise; and $\{\theta\}, \theta_i, i = 1, ..., n_u$ lying in $\Theta \in R^{n_u}$ is the vector that represents the uncertain system parameters involved in the problem. The uncertain system parameters $\{\theta\}$ are modeled using a prescribed probability density function $q(\{\theta\}|\{\phi\})$ that incorporates available knowledge about the system. For structural systems under stochastic excitation the multidimensional integral [Eq. (4)], in general, involves a large number of uncertain parameters (in the order of thousands). Therefore, the reliability estimation for a given design constitutes a high dimensional problem that is extremely demanding from a numerical point of view. A model prediction error—that is, the error between the response of the actual system and the response of the model—also can be considered in the formulation [15, 16]. In this case the prediction error may be modeled probabilistically by augmenting the vector $\{\theta\}$ to form an uncertain parameter vector composed of both system model parameters as well as model prediction errors. The failure domain $\Omega_{F_j}(\{\phi\})$ corresponding to the failure event F_j evaluated at the design $\{\phi\}$ is described in terms of a performance function g_j as

$$\Omega_{F_j}(\{\phi\}) = \{\{\theta\} \mid g_j(\{\phi\}, \{\theta\}) \leq 0\} \tag{5}$$

Then, the probability of failure also can be expressed in terms of the failure domain in the form

$$P_{F_j}(\{\phi\}) = \int_{\Omega_{F_j}(\{\phi\})} q(\{\theta\}|\{\phi\}) d\{\theta\} \tag{6}$$

With the previous notation, a reliability constraint can be written as

$$h_j(\{\phi\}) = P_{F_j}(\{\phi\}) - P^*_{F_j} \leq 0 \tag{7}$$

where $P^*_{F_j}$ is the target failure probability. The last inequality expresses the requirement that the probability of system failure must be smaller than an appropriate tolerance. It is noted that in the context of stochastic design a system that corresponds to a feasible design cannot be certified with complete certainty, but with a tolerance $P^*_{F_j}$. In other words, the system will operate safely within the pre-specified probability of failure tolerance.

3. PHYSICAL MODEL

Base-isolated systems are designed such that the superstructure remains elastic. Hence, the structure is modeled as a linear elastic system in the present formulation. The base and the floors are assumed to be infinitely rigid in plane. The superstructure and the base are modeled using three degrees of freedom per floor at the center of mass. Each nonlinear isolation element is modeled explicitly using the Buoc-Wen model [8]. Let $\{x_s(t)\}$ be the nth dimensional vector of absolute displacements for the superstructure with respect to the base and $[M_s]$, $[C_s]$, and $[K_s]$ be the corresponding mass, damping, and stiffness matrices. Also, let $\{x_b(t)\}$ be the vector of base displacements with three components and $[G_s]$ be the matrix of earthquake influence coefficients of dimension $n \times 3$; that is, the matrix that couples the excitation components of the vector $\{\ddot{x}_g(t)\}$ to the degrees of freedom of the superstructure. The equation of motion of the elastic superstructure then is expressed in the form

$$[M_s]\{\ddot{x}_s(t)\} + [C_s]\{\dot{x}_s(t)\} + [K_s]\{x_s(t)\} = -[M_s][G_s](\{\ddot{x}_b(t)\} + \{\ddot{x}_g(t)\}) \tag{8}$$

where $\{\ddot{x}_b(t)\}$ is the vector of base accelerations relative to the ground. On the other hand, the equation of motion of the base can be written as

$$([G_s]^T[M_s][G_s] + [M_b])(\{\ddot{x}_b(t)\} + \{\ddot{x}_g(t)\}) + [G_s]^T[M_s]\{\ddot{x}_s(t)\} + \{f_{is}\} = \{0\} \tag{9}$$

where $[M_b]$ is the diagonal mass matrix of the rigid base and $\{f_{is}\}$ is the vector containing the nonlinear isolation element forces (three components). The characterization of such forces is treated in a subsequent section. Rewriting the previous equations, the combined equation of motion of the base-isolated structural system can be formulated in the form

$$\begin{aligned} &\begin{bmatrix} [M_s] & [M_s][G_s] \\ [G_s]^T[M_s] & [M_b] + [G_s]^T[M_s][G_s] \end{bmatrix} \begin{Bmatrix} \{\ddot{x}_s(t)\} \\ \{\ddot{x}_b(t)\} \end{Bmatrix} + \begin{bmatrix} [C_s] & [0] \\ [0]^T & [0] \end{bmatrix} \begin{Bmatrix} \{\dot{x}_s(t)\} \\ \{\dot{x}_b(t)\} \end{Bmatrix} \\ &+ \begin{bmatrix} [K_s] & [0] \\ [0]^T & [0] \end{bmatrix} \begin{Bmatrix} \{x_s(t)\} \\ \{x_b(t)\} \end{Bmatrix} = - \begin{Bmatrix} [M_s][G_s] \\ [M_b] + [G_s]^T[M_s][G_s] \end{Bmatrix} \{\ddot{x}_g(t)\} - \begin{Bmatrix} \{0\} \\ \{f_{is}(t)\} \end{Bmatrix} \end{aligned} \tag{10}$$

4. STOCHASTIC EXCITATION MODEL

4.1 Point-Source Stochastic Method

The ground acceleration is modeled as a nonstationary stochastic process. In particular, a point-source model characterized by the moment magnitude M and epicentral distance r is considered here [7, 17]. The model is a simple, yet powerful, means for simulating ground motions and it has been successfully applied in the context of seismic engineering. The time history of the ground acceleration for a given magnitude M and epicentral distance r is obtained by modulating a white noise sequence by an envelope function and, subsequently, by a ground motion spectrum through the following steps:

1. Generate a discrete-time Gaussian white noise sequence with unitary intensity

$$\omega(t_j) = \sqrt{1/\Delta t}\, \theta_j \ , j = 1, ..., n_T \tag{11}$$

where $\theta_j, j = 1, ..., n_T$, are independent, identically distributed standard Gaussian random variables; Δt is the sampling interval; and n_T is the number of time instants equal to the duration of the excitation T divided by the sampling interval.

2. The white noise sequence is modulated by an envelope function $e(t, M, r)$ at the discrete time instants.

3. Discrete Fourier transform is applied to the the modulated white noise sequence.

4. The resulting spectrum is normalized by the square root of the average square amplitude spectrum.

5. The normalized spectrum is multiplied by a ground motion spectrum (or radiation spectrum) $S(f, M, r)$ at discrete frequencies $f_l = l/T, l = 1, ..., n_T/2$.

6. Discrete inverse Fourier transform is applied to transform the sequence back to the time domain to yield the desired ground acceleration time history.

Thus, the synthetic ground motion generated from the model is a function of the independent, identically distributed standard Gaussian random variables $\theta_j, j = 1, ..., n_T$ and the stochastic excitation model parameters M and r. Details of the characterization of the envelope function $e(t, M, r)$ and the ground acceleration spectrum $S(f, M, r)$ are provided in the subsequent sections. It is noted that this excitation model is well suited for generating the high-frequency components of the ground motion. Low-frequency components also can be introduced in the analysis by combining the above methodology with near-fault ground motion models [18].

4.2 Seismicity Model

The probabilistic model for the seismic hazard at the emplacement is complemented by considering that the moment magnitude M and epicentral distance r are also uncertain. The uncertainty in moment magnitude is modeled by the Gutenberg-Richter relationship truncated on the interval $[6.0, 8.0]$, which leads to the probability density function [19]

$$p(M) = \frac{b\, e^{-bM}}{e^{-6.0b} - e^{-8.0b}} \quad , \quad 6.0 \leq M \leq 8.0 \tag{12}$$

where b is a regional seismicity factor. For the uncertainty in the epicentral distance r, a log-normal distribution with mean value $\bar{r}$ (km) and standard deviation σ_r (km) is used.

4.3 Envelope Function

The envelope function for the ground acceleration is represented by [7, 20]

$$e(t, M, r) = a_1 \left(\frac{t}{t_n}\right)^{a_2} e^{-a_3(t/t_n)} \tag{13}$$

where

$$a_2 = \frac{-0.2\ln(0.05)}{1 + 0.2(\ln(0.2) - 1)} \ , \ a_3 = \frac{a_2}{0.2} \ , \ a_1 = \left(\frac{e^1}{0.2}\right)^{a_2} \tag{14}$$

The envelope function has a peak equal to unity when $t = 0.2\ t_n$, and $e(t, M, r) = 0.05$ when $t = t_n$, with $t_n = 2.0\ T_{gm}$, where T_{gm} is the duration of ground motion, expressed as a sum of a path-dependent and source-dependent component $T_{gm} = 0.05\sqrt{r^2 + h^2} + 0.5/f_a$, where r is the epicentral distance, and the parameters h and f_a (corner frequency) are moment dependent given by $\log(h) = 0.15M - 0.05$ and $\log(f_a) = 2.181 - 0.496M$ [17].

4.4 Ground Motion Spectrum

The total spectrum of the motion at a site $S(f, M, r)$ is expressed as the product of the contribution from the earthquake source $E(f, M)$, path $P(f, r)$, site $G(f)$, and type of motion $I(f)$; i.e.,

$$S(f, M, r) = E(f, M)\ P(f, r)\ G(f)\ I(f) \tag{15}$$

The source component is given by

$$E(f, M) = C\ M_0(M)\ S_a(f, M) \tag{16}$$

where C is a constant, $M_0(M) = 10^{1.5M+10.7}$ is the seismic moment, and the factor S_a is the displacement source spectrum given by [17]

$$S_a(f, M) = \frac{1-\varepsilon}{1+(f/f_a)^2} + \frac{\varepsilon}{1+(f/f_b)^2} \tag{17}$$

where the corner frequencies f_a and f_b, and the weighting parameter ε are defined, respectively, as $\log(f_a) = 2.181 - 0.496M$, $\log(f_b) = 2.41 - 0.408M$, and $\log(\varepsilon) = 0.605 - 0.255M$. The constant C is given by $C = UR_\Phi VF/4\pi\rho_s\beta_s^3 R_0$, where U is a unit-dependent factor, R_Φ is the radiation pattern, V represents the partition of total shear-wave energy into horizontal components, F is the effect of the free surface amplification, ρ_s and β_s are the density and shear-wave velocity in the vicinity of the source, and R_0 is a reference distance. Next, the path effect $P(f, r)$, which is another component of the process that affects the spectrum of motion at a particular site, is represented by functions that account for geometrical spreading and attenuation

$$P(f, r) = Z[R(r)]\ e^{-\pi f R(r)/Q(f)\beta_s} \tag{18}$$

where $R(r)$ is the radial distance from the hypocenter to the site given by $R(r) = \sqrt{r^2 + h^2}$. The attenuation quantity $Q(f)$ is taken as $Q(f) = 180f^{0.45}$ and the geometrical spreading function is selected as $Z[R(r)] = 1/R(r)$ if $R(r) < 70.0$ km and $Z[R(r)] = 1/70.0$ otherwise [17]. The modification of seismic waves by local conditions, site effect $G(f)$, is expressed by the multiplication of a diminution function $D(f)$ and an amplification function $A(f)$. The diminution function accounts for the path-independent loss of high frequency in the ground motions and can be accounted for a simple filter of the form $D(f) = e^{-0.03\pi f}$?. The amplification function $A(f)$ is based on empirical curves given in [22] for generic rock sites. An average constant value equal to 2.0 is considered. Finally, the filter that controls the type of ground motion $I(f)$ is chosen as $I(f) = (2\pi f)^2$ for ground acceleration. The particular values of the different parameters of the stochastic ground acceleration model used in this work are given in Table 1. For illustration purposes. Figure 1 shows the envelope function, the ground motion spectrum and a corresponding sample of ground motion for a nominal distance $r = 20$ km, and moment magnitude $M = 7.0$. For a detaied discussion of this point-source model the reader is referred to [17, 22].

As previously pointed out, the excitation model considered in this work is based on a class of point-source models. In this regard it is important to note that the proposed methodology for robust design of base-isolated structural systems is not limited in any way to this particular model. For example, excitation models based on second-order processes, filtered white noise sequences, and spectral representations can be used as well. The particular model to be used will depend, among other things, on the available seismic information at the site where the structural system is situated.

TABLE 1: Parameters for the stochastic ground acceleration model

Parameter	Numerical Value	Parameter	Numerical Value
$\bar{r}$ (km)	20.0	σ_r (km)	9.0
b	1.8	U	10^{-20}
ρ_s (gm/cc)	2.8	β_s (km/s)	3.5
V	$1/\sqrt{2}$	R_Φ	0.55
F	2.0	R_0 (km)	1.0
T (s)	20.0	Δt (s)	0.01

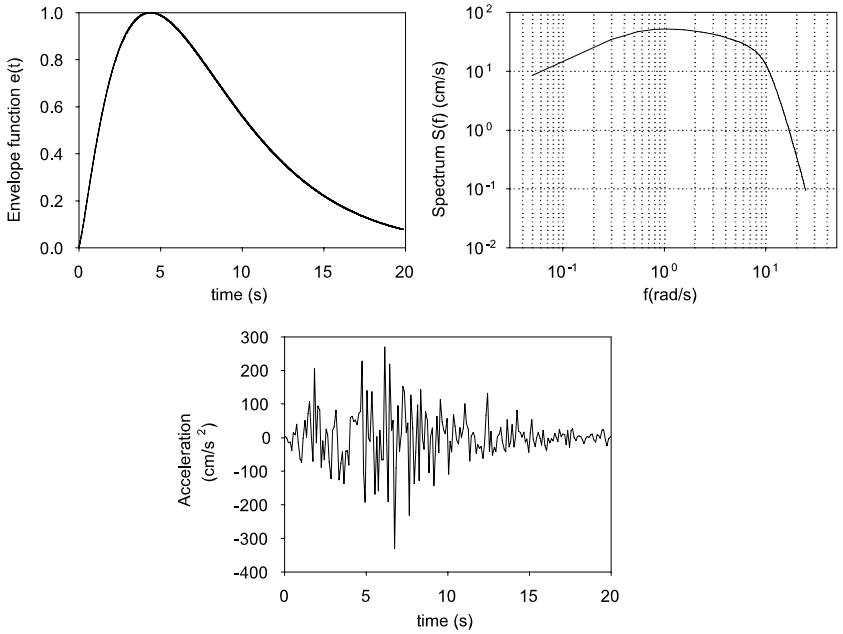

FIG. 1: Envelope function, ground acceleration spectrum, and sample ground motion for M = 7.0 and r = 20 (km).

5. ISOLATION MODEL

Several isolation elements can be used to model isolation systems. They include elastic, viscous, nonlinear fluid dampers, hysteretic (uniaxial or biaxial) elements for bilinear elastomeric bearings, hysteretic (uniaxial or biaxial) elements for sliding bearings, etc. Uniaxial bearings with hysteretic behavior, such as lead rubber bearings, are used in the present implementation. The behavior of the bearings is characterized by the Buoc-Wen model as [8]

$$U^y\ \dot{z}(t) = \begin{cases} \dot{x}_b(t)(\alpha - z^n(t)\{\gamma\ \text{sgn}[\dot{x}_b(t)z(t)] + \beta\}) & \text{if n is even} \\ \dot{x}_b(t)(\alpha - z^n(t)\{\gamma\ \text{sgn}[\dot{x}_b(t)] + \beta\ \text{sgn}[z(t)]\}) & \text{if n is odd} \end{cases} \tag{19}$$

where $z(t)$ is a dimensionless hysteretic variable; α, β, and γ are dimensionless quantities; U^y is the yield displacement; $x_b(t)$ and $\dot{x}_b(t)$ represent the base displacement and velocity, respectively; and sgn$(\cdot)$ is the sign function. The forces activated in the isolation bearing are modeled by an elastic-viscoplastic model with strain hardening

$$f_{is}(t) = \alpha_L k_e\ x_b(t)\ +\ c_v\ \dot{x}_b(t)\ +\ (1-\alpha_L)k_e\ \ U^y\ z(t) \tag{20}$$

where k_e is the pre-yield stiffness, c_v is the viscous damping coefficient of the isolation element, U^y is the yield displacement, and α_L is a factor that defines the extent to which the force is linear.

6. SEQUENTIAL APPROXIMATE OPTIMIZATION

6.1 Approximate Sub-Optimization Problem

The solution of the stochastic optimization problem given by Eqs. (1)–(3) is obtained by transforming it into a sequence of sub-optimization problems having a simple explicit algebraic structure. Thus, the strategy is to construct successive approximate analytical sub-problems. To this end, the objective and the constraint functions are represented by using approximate functions dependent on the design variables. In particular, a hybrid form of linear, reciprocal, and quadratic approximations is considered in the present formulation [10, 23, 24]. At the kth iteration the approximate discrete sub-optimization problem takes the form

$$\text{Minimize}\ \ \tilde{f}_k(\{\phi\}) \tag{21}$$

subject to

$$\tilde{h}_{jk}(\{\phi\}) \leq 0 \ , \ \ j = 1, ..., n_c \tag{22}$$

with side constraints

$$\{\phi\} \in \Phi \tag{23}$$

where $\tilde{f}_k$ and $\tilde{h}_{jk}, j = 1, ...n_c$ represent the approximate objective and constraint functions at the current point $\{\phi^k\}$ in the design space, respectively. The approximate objective function is obtained as

$$\tilde{f}_k(\{\phi\}) = f_{1k}(\{\phi\}) + f_{2k}(\{\phi\}) + f_{3k}(\{\phi\}) \tag{24}$$

where $f_{1k}(\{\phi\})$ is a linear function in terms of the design variables, $f_{2k}(\{\phi\})$ is a linear function with respect to the inverse of the design variables, and $f_{3k}(\{\phi\})$ is a quadratic function of the design variables. They are given by

$$f_{1k}(\{\phi\}) = \sum_{(i^+)} \frac{\partial f(\{\phi^k\})}{\partial \phi_i} \phi_i \ \ , \ \ f_{2k}(\{\phi\}) = -\sum_{(i^-)} \frac{\partial f(\{\phi^k\})}{\partial \phi_i} \frac{(\phi_i^k)^2}{\phi_i} \tag{25}$$

$$f_{3k}(\{\phi\}) = -2\chi^f \sum_{(i^-)} \frac{\partial f(\{\phi^k\})}{\partial \phi_i} \phi_i \left(\frac{\phi_i}{\phi_i^k} - 2 \right) \tag{26}$$

where (i^+) is the group that contains the variables for which the partial derivative of the objective function is positive and (i^-) is the group that includes the remaining variables. On the other hand, the constraint functions involving reliability measures (reliability constraints) are first transformed as $h_j^t(\{\phi\}) = Ln[P_{F_j}(\{\phi\})]$. Then, the transformed constraint functions at the kth iteration are approximated in the form

$$\tilde{h}_{jk}^t(\{\phi\}) \ = h_{j1k}^t(\{\phi\}) + h_{j2k}^t(\{\phi\}) + h_{j3k}^t(\{\phi\}) + \bar{h}_{jk}^t(\{\phi^k\}) \tag{27}$$

with

$$h_{j1k}^t(\{\phi\}) = \sum_{(i_j^+)} \frac{\partial h_j^t(\{\phi^k\})}{\partial \phi_i} \phi_i \ \ , \ \ h_{j2k}^t(\{\phi\}) = -\sum_{(i_j^-)} \frac{\partial h_j^t(\{\phi^k\})}{\partial \phi_i} \frac{(\phi_i^k)^2}{\phi_i} \tag{28}$$

$$h_{j3k}^t(\{\phi\}) = 2\chi^{h_j^t} \sum_{(i_j^-)} \frac{\partial h_j^t(\{\phi^k\})}{\partial \phi_i} \phi_i \left(\frac{\phi_i}{\phi_i^k} - 2 \right) \tag{29}$$

$$\bar{h}_{jk}^t(\{\phi^k\}) = h_j^t(\{\phi^k\}) - \sum_{(i_j^+)} \frac{\partial h_j^t(\{\phi^k\})}{\partial \phi_i} \phi_i^k - (2\chi^{h_j^t} - 1) \sum_{(i_j^-)} \frac{\partial h_j^t(\{\phi^k\})}{\partial \phi_i} \phi_i^k \tag{30}$$

where $\sum_{(i_j^+)}$ and $\sum_{(i_j^-)}$ mean summation over the variables belonging to group (i_j^+) and (i_j^-), respectively. Group (i_j^+) contains the variables for which $\partial h_j^t(\{\phi^k\})/\partial \phi_i$ is positive and group (i_j^-) includes the remaining variables. The same type of approximations can be applied to the deterministic constraint functions. In the above expressions the parameters χ^f and $\chi^{h_j^t}$ are user-defined positive scalars that control the conservatism of the approximations [25].

6.2 Solution Scheme

The solution scheme of the optimization process is summarized as follows:

1. At the beginning of the kth design cycle ($k = 0, 1, 2, ...$) the objective function f and constraint functions $h_j, j = 1, ..., n_c$ are approximated by using the approach defined in the previous section. The approximations require function evaluations [$f(\{\phi^k\})$, $h_j^t(\{\phi^k\}), j = 1, ..., n_c$] and sensitivity analyses [$\nabla f(\{\phi^k\})$, $\nabla h_j^t(\{\phi^k\}), j = 1, ..., n_c$].

2. Using this information an explicit sub-optimization problem is constructed. The explicit problem is solved by standard methods that treat the problem directly in the primal design variables space to arrive at the design $\{\phi^{*k}\}$.

3. The new point $\{\phi^{*k}\}$ is tested if it is acceptable in terms of a conservative criterion; that is, if $\tilde{f}_k(\{\phi^{*k}\}) \geq f(\{\phi^{*k}\})$ and if $\tilde{h}^t_{jk}(\{\phi^{*k}\}) \geq h^t_j(\{\phi^{*k}\}), j = 1, ...n_c$. If these conditions are satisfied (conservative step) the point $\{\phi^{*k}\}$ is used as the current design for the next cycle; that is, $\{\phi^{k+1}\} = \{\phi^{*k}\}$. If the design $\{\phi^{*k}\}$ does not represent a conservative step an inner loop is initiated to affect conservatism. For functions that are not conservative at $\{\phi^{*k}\}$ the corresponding coefficients of the second-order terms are increased by multiplying the corresponding scalar χ by a constant greater than 1. The modified approximations are used to construct a new sub-optimization problem to obtain a new point. It is noted that the conservatism of the approximations affects the global convergence of the optimization process [11, 25, 26]. It ensures that the optimal solution of the sub-optimization problem is a feasible solution of the original problem.

4. The design process is continued until some convergence criterion is satisfied.

The requirement of a conservative step in the above algorithm can be relaxed and demand that a feasible descent step is made instead; i.e., if $f(\{\phi^{*k}\}) < f(\{\phi^{*(k-1)}\})$ and if $h^t_j(\{\phi^{*k}\}) \leq \ln[P^*_{F_j}], j = 1, ...n_c$. In this case, the conservatism is only enforced when a feasible descent step could not be made. This approach, which is called relaxed conservatism, inherits the global convergence properties of the algorithm that enforces conservatism at each design cycle [26]. The level of effectiveness of the above sequential optimization scheme depends on the degree of convexity of the functions involved in the optimization problem. For example, if the curvatures are not too large and relatively uniform throughout the design space the proposed algorithm converges within a few iterations [12, 27]. For more general cases, methods based on trust regions and line search methodologies may be more appropriate [28–30].

7. IMPLEMENTATION ASPECTS

7.1 Exterior Sampling Approximation

Solution approaches to optimization problems using stochastic simulation are based on either interior or exterior sampling techniques [31]. In the present formulation an exterior sampling approximation is adopted. The approach uses the same stream of random numbers throughout all iterations in the optimization process. Thus, the approximate optimization problem [Eq. (21)–(23)] is transformed into a deterministic one. It is noted that several asymptotic results are available for exterior sampling techniques and their rate of convergence under weak assumptions [32]. For finite-dimensional sample sizes, the final solution depends on the sample selected; i.e., $\Theta_N = [\{\theta_1\}, \{\theta_2\}, ..., \{\theta_N\}]$, where the N samples of the uncertain parameters are drawn from the probability density function $q(\{\theta\}|\{\phi\})$. In order to get good quality estimates for the reliability measures—and, thus, accurate solution to the optimization problem—the exterior sampling approximation is implemented by selecting N sufficiently large. A scheme that considers higher accuracy estimates as the algorithm converges to the final solution is implemented in the present formulation. In addition, the average of several independent estimations of the failure probability is considered for controlling the variability of the estimators. Numerical validations have indicated that for the class of problems considered in the context of this study only a small number of independent simulation runs is required to obtain the estimates with sufficient accuracy. For the general case, the number of simulation runs needs to be established for the particular type of problems under consideration.

7.2 Reliability Estimation

The reliability constraint functions $h_j(\{\phi\}), j = 1, ..., n_c$ defined in Eq. (7) are given in terms of the first excursion probability functions $P_{F_j}(\{\phi\}), j = 1, ..., n_c$. Subset simulation is adopted in this formulation for the purpose of estimating the corresponding failure probabilities during the design process [9]. In the approach, the failure probabilities are expressed as a product of conditional probabilities of some chosen intermediate failure events, the evaluation of which only requires simulation of more frequent events. Therefore, a rare event simulation problem is converted

into a sequence of more frequent event simulation problems. For example, the failure probability $P_{F_j}(\{\phi\})$ can be expressed as the product

$$P_{F_j}(\{\phi\}) \;=\; P(F_{j,1}(\{\phi\}))\;\prod_{k=1}^{m_{F_j}-1}\;P[F_{j,k+1}(\{\phi\})/F_{j,k}(\{\phi\})] \tag{31}$$

where $P[(\cdot)]$ denotes the probability of occurrence, $F_{j,m_{F_j}}(\{\phi\}) = F_j(\{\phi\})$ is the target failure event, and

$$F_{j,m_{F_j}}(\{\phi\}) \subset F_{j,m_{F_j}-1}(\{\phi\}) \subset ... \subset F_{j,1}(\{\phi\}) \tag{32}$$

is a nested sequence of failure events. Equation (31) expresses the failure probability $P_{F_j}(\{\phi\})$ as the product of $P[F_{j,1}(\{\phi\})]$ and the conditional probabilities $P[F_{j,k+1}(\{\phi\})/F_{j,k}(\{\phi\})]$, $k = 1, ..., m_{F_j} - 1$. It is seen that, even if $P_{F_j}(\{\phi\})$ is small, by choosing m_{F_j} and $F_{j,k}(\{\phi\}), k = 1, ..., m_{F_j} - 1$ appropriately, the conditional probabilities still can be made sufficiently large and, therefore, they can be evaluated efficiently by simulation because the failure events are more frequent. The intermediate failure events are chosen adaptively using information from simulated samples so that they correspond to some specified values of conditional failure probabilities. Then, to compute $P_{F_j}(\{\phi\})$ based on Eq. (31) one needs to estimate the probabilities $P[F_{j,1}(\{\phi\})]$ and $P[F_{j,k+1}(\{\phi\})/F_{j,k}(\{\phi\})]$, $k = 1, ..., m_{F_j} - 1$. The probability $P[F_{j,1}(\{\phi\})]$ can be estimated readily by Monte Carlo as

$$P[F_{j,1}(\{\phi\})] \approx \tilde{P}[F_{j,1}(\{\phi\}), \Theta_N] = \frac{1}{N}\sum_{k=1}^{N} I_{F_{j,1}}(\{\phi\}, \{\theta_k\}) \tag{33}$$

where $\Theta_N = [\{\theta_1\}, \{\theta_2\}, ..., \{\theta_N\}]$ are independent and identical distributed samples simulated according to the probability density function $q(\{\theta\} \mid \{\phi\})$. On the other hand, the conditional failure probability $P[F_{j,k+1}(\{\phi\})/F_{j,k}(\{\phi\})]$ is estimated in a similar manner; i.e.,

$$P[F_{j,k+1}(\{\phi\})/F_{j,k}(\{\phi\})] \approx \tilde{P}[F_{j,k+1}(\{\phi\})/F_{j,k}(\{\phi\}), \Theta_N] = \frac{1}{N}\sum_{k=1}^{N} I_{F_{j,k+1}}(\{\phi\}, \{\theta_k\}) \tag{34}$$

with samples according to the conditional distribution of $\{\theta\}$ given that it lies in $F_{j,k}$; that is, samples $\{\theta_k\}$ simulated according to $q(\{\theta\}|F_{j,k}, \{\phi\})$. It is noted that the direct generation of samples simulated from q, which lie in the failure region $F_{j,k}$, is not efficient since on the average it takes $1/P[F_{j,k}(\{\phi\})]$ samples before one such sample occurs. In view of this difficulty the conditional samples are generated by an efficient Markov chain Monte Carlo method based on the Metropolis algorithm [9, 33]. The probabilities are estimated using $N = 500$ samples during the initial iterations of the optimization process. This number is increased to $N = 1000$ as the algorithm converges to the final solution. Validation calculations have shown that subset simulation can be applied efficiently to first excursion problems for a wide range of dynamical systems, including the systems considered in this study. For a detailed discussion of the approach the reader is referred to [9].

7.3 Sensitivity Estimation

It is clear that the characterization of the approximate optimization problems [Eqs. (21)–(23)] requires the estimation of the sensitivity of the transformed failure probability functions. The sensitivity of the transformed failure probability functions with respect to the design variables is estimated by an approach recently introduced in [34]. The approach is based on the approximate representation of two different quantities. The first approximation involves the performance function while the second includes the failure probability function. For completeness, the basic ideas of the methodology are presented below. Recall that the failure domain Ω_{F_j} for a given design $\{\phi\}$ is defined as $\Omega_{F_j}(\{\phi\}) = \{\{\theta\} \mid g_j(\{\phi\}, \{\theta\},) \leq 0\}$. If $\{\phi^k\}$ is the current design, the performance function g_j is approximated in the vicinity of the current design as

$$\bar{g}_j(\{\phi\}, \{\theta\}) = g_j(\{\phi^k\}, \{\theta\}) + \{\delta g_j\}^T\{\Delta\phi\} \tag{35}$$

where $\{\phi\} = \{\phi^k\} + \{\Delta\phi\}$. The evaluation of the coefficients $\{\delta g_j\}$ is carried out in two steps:

1. In a first step, for samples $\{\theta_i\}, i = 1, ..., M$ near the limit state surface—that is, $g_j(\{\phi\}, \{\theta_i\}) \approx 0$—the performance function is evaluated at points in the neighborhood of $\{\phi^k\}$. These points are generated as

$$\{\phi^{pk}\} - \{\phi^k\} = \{\Delta\phi\} = \frac{\{\xi_p\}}{\parallel \{\xi_p\} \parallel} R \ , \ p = 1, ..., Q \times M \tag{36}$$

   where the components of the vector $\{\xi_p\}$ are independent, identically distributed standard Gaussian random variables; Q is a positive integer and R is a user-defined small positive number. This number defines the radius of the hypersphere $\{\xi_p\}/ \parallel \{\xi_p\} \parallel R$ centered at the current design $\{\phi^k\}$.

2. In a second step, the coefficients $\{\delta g_j\}$ of the approximation (35) are computed by least squares. To this end, the following set of equations is generated

$$\begin{aligned} g_j(\{\phi^{pk}\}, \{\theta_i\}) = g_i(\{\phi^k\}, \{\theta_i\}) + \{\delta g_j\}^T \frac{\{\xi_p\}}{\parallel \{\xi_p\} \parallel} R \\ p = i + (q-1) \times M \ , q = 1, ..., Q \ , i = 1, ..., M \end{aligned} \tag{37}$$

Since the samples $(\{\theta_i\}), i = 1, ..., M$ are chosen near the limit state surface the approximate performance function $\bar{g}_j$ is expected to be representative, on the average, of the behavior of the failure domain Ω_{F_j} in the vicinity of the current design $\{\phi^k\}$ [30]. Numerical experience has shown that the approximation introduced in Eq. (35) is adequate in the context of the proposed optimization scheme. Issues such as the number of points required for performing least square (Q and M), and the generation of design points in the vicinity of the current design (calibration of the radius R) are discussed in [34].

Next, the failure domain Ω_{F_j} for a given design $\{\phi\}$ is defined in terms of the normalized demand function as $\Omega_{F_j}(\{\phi\}) = \{\{\theta\} \mid D_j(\{\phi\}, \{\theta\}) \geq 1\}$ where $D_j(\{\phi\}, \{\theta\}) = 1 - g_j(\{\phi\}, \{\theta\})$. The failure probability function, evaluated at the current design $\{\phi^k\}$, is then approximated locally as an explicit function of the normalized demand around $D_j^* = 1$ as

$$\begin{aligned} P\left[D_j(\{\phi^k\}, \{\theta\}) \geq D_j^*\right] \approx e^{\psi_0 + \psi_1 (D_j^* - 1)} \\ D_j^* \ \in \ [1 - \epsilon, 1 + \epsilon] \end{aligned} \tag{38}$$

where D_j^* is a threshold of the normalized demand (in the neighborhood of 1) and ϵ represents a small tolerance. The coefficient ψ_0 corresponds to the probability of failure $P_{F_j}(\{\phi^k\})$ and the coefficient ψ_1 can be calculated by least squares with samples generated at the last stage of subset simulation [9, 30, 34]. The sensitivity of the jth failure probability function can be estimated by means of the limit:

$$\left.\frac{\partial P_{F_j}(\{\phi\})}{\partial \phi_l}\right|_{\{\phi\}=\{\phi^k\}} = \lim_{\Delta\phi_l \to 0} \frac{P_{F_j}(\{\phi^k\} + \{\delta(l)\}\Delta\phi_l) - P_{F_j}(\{\phi^k\})}{\Delta\phi_l} \qquad l = 1, \ldots, n_d \tag{39}$$

where n_d is the total number of design variables and $\{\delta(l)\}$ is a vector of length n_d with all entries equal to zero, except by the lth entry, which is equal to 1. Considering the definition of failure probability in terms of the normalized demand function, the linear expansion of the performance function in Eq. (35), and the approximation of the failure probability function given in Eq. (38), the partial derivative of the jth transformed failure probability function $\{h_j^t(\{\phi\}) = \ln[P_{F_j}(\{\phi\})]\}$ can be expressed as

$$\left.\frac{\partial h_j^t(\{\phi\})}{\partial \phi_l}\right|_{\{\phi\}=\{\phi^k\}} \approx \frac{1}{P_{F_j}(\{\phi^k\})} \times \lim_{\Delta\phi_l \to 0} \frac{e^{\psi_0 + \psi_1 \delta g_{jl} \Delta\phi_l} - e^{\psi_0}}{\Delta\phi_l} = \psi_1 \delta g_{jl} \qquad l = 1, \ldots, n_d$$

where δg_{jl} is the lth element of the vector $\{\delta g_j\}$, and all other terms have been previously defined. It is noted that the previous approach for estimating the gradients of the failure probability functions requires a single reliability analysis plus the evaluation of the performance functions in the vicinity of the current design. Validation calculations have shown that this approach is quite efficient for estimating the sensitivity of failure probability functions with respect to design variables. It is important to note that the proposed sensitivity analysis attempts to generate metrics that can approximate the gradient of the failure probability functions (whenever they exist) or provides information on the local sensitivity of the failure probability functions in cases where the associated gradient does not exist.

8. NUMERICAL EXAMPLE

8.1 Description

A 10-story reinforced concrete (RC) frame including a base-isolation system (composed of lead rubber bearings) subject to a stochastic ground acceleration is considered as a numerical example. A schematic representation of the model is shown in Fig. 2. The frame can be considered as one resistant element of the three-dimensional model characterized in Section 3. Each floor of the RC frame is supported by six columns of square shape and a height of 3 m leading to a total height of 30 m. It is assumed that the beams of the frame are rigid in the axial direction, so each floor can be described by a single horizontal degree of freedom. As previously pointed out (see Section 3 on the physical model), the frame structure remains linear throughout the duration of the ground acceleration. The Young's modulus is equal to 3×10^{10} N/m^2. The mass of each floor is equal to 1.5×10^5 kg, while the mass of the base is equal to 3.0×10^5 kg. A 5% critical damping is assumed in the model. The base-isolation system is composed of six uniaxial lead rubber bearings with hysteretic behavior. The nonlinear behavior of these devices is modeled by the equation described in Section 5 with model parameters $n = 1$, $\alpha = 1.0$, $\beta = -0.65$, $\gamma = 0.5$, $U^y = 0.5$ cm, $\alpha_L = 0.1$, $k_e = 3 \times 10^6$ N/m, and $c_v = 0.0$. Figures 3 and 4 show a schematic representation of a lead rubber bearing and a typical displacement-restoring force curve of the isolation element, respectively. The structural system is excited horizontally by a ground acceleration that is modeled as described in Section 4. For clarity and simplicity all structural parameters are assumed to be known in this case. Therefore, the uncertain system parameters involved in this problem are represented by the stochastic excitation model parameters. However, it is emphasized that the effect of uncertain structural parameters can be considered directly by the methodology proposed in the previous sections.

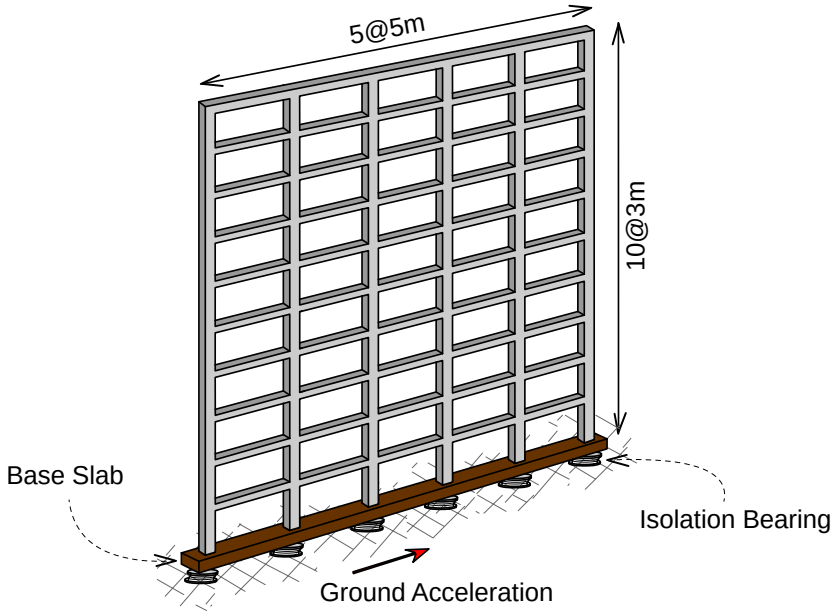

FIG. 2: Ten-story RC frame with base-isolation system.

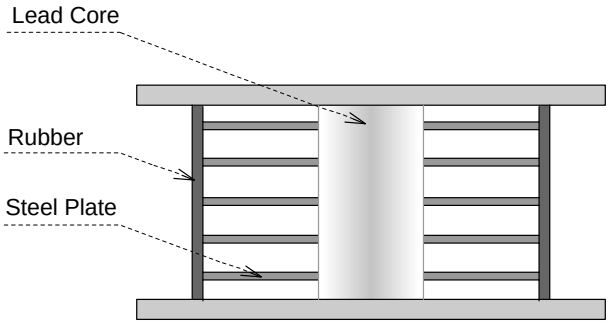

FIG. 3: Lead rubber bearing.

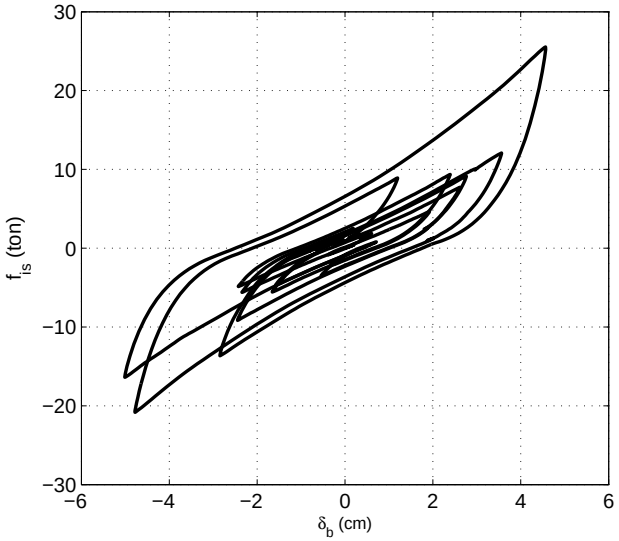

FIG. 4: Typical displacement-restoring force curve of the isolation element (lead rubber bearings).

8.2 Stochastic Design Problem

The objective function f is defined as the total area of the column elements of the frame. The design variables $\{\phi\}$ are chosen as the inertia of the columns throughout the height, grouped in 10 design variables; i.e., the inertia of the columns of each floor constitutes each of the design groups. The failure events are formulated as first passage problems. The structural responses to be controlled are the 10 interstory drift displacements. Thus, the failure domains evaluated at the design $\{\phi\}$ are given by

$$\Omega_{F_j}(\{\phi\}) = \{\{\theta\} \mid \max_{t_k, k=1,..,2000} |\delta_j(t_k, \{\phi\}, \{\theta\})| - \delta^* \geq 0\} \ , \ \ j = 1, ..., 10 \tag{40}$$

where $\delta_j(t_k, \{\phi\}, \{\theta\})$ is the relative displacement between the $(j-1, j)$th floor evaluated at the design $\{\phi\}$, t_k are the discrete time instants, δ^* is the critical threshold level and equal to 0.2% of the floor height, and $\{\theta\}$ is the vector that represents the uncertain system parameters (stochastic excitation model). Note that the duration of the excitation is 20 s and the sampling interval is equal to 0.01 s (see Table 1). Therefore, the vector $\{\theta\}$ has 2000 components. This, in turn, implies that the estimation of the failure probability for a given design represents a high dimensional reliability problem [see Eq. (4)]. The tolerable probability of failure (P_F^*) is set equal to 10^{-3}. Additionally, geometric and side constraints are incorporated in the problem. The reliability-based optimization problem is defined as

$$\text{Min } f(\{\phi\})$$

subject to

$$\begin{aligned} P_{F_j}(\{\phi\}) - P_F^* &\le 0, j = 1, \ldots, 10 \\ \phi_{i+1} - \phi_i &\le 0,\ i = 1, \ldots, 9 \\ -\phi_i + 5.0 \times 10^{-3} &\le 0,\ i = 1, \ldots, 10 \\ \phi_i - 7.0 \times 10^{-2} &\le 0,\ i = 1, \ldots, 10 \end{aligned} \tag{41}$$

8.3 Results

The initial design is shown in Table 2. The results of the optimization procedure are presented in Fig. 5 in terms of the evolution of the objective function. It is observed that only a few optimization cycles are required for obtaining convergence. In fact, most of the improvement of the objective function takes place in the first three optimization cycles. Then, the design process takes few excursion probability and sensitivity estimations. The details on the optimization procedure for the initial design and the final design are summarized in Table 2. The numerical results also show that the method generates a series of steadily improved feasible designs that move toward the optimum. This property is important from a practical viewpoint since the design process may be stopped at any stage still leading

TABLE 2: Initial and final designs

Design variables	Initial design	Final design
$\phi_1 \times 10^{-2}$ (m^4)	5.4	4.7
$\phi_2 \times 10^{-2}$ (m^4)	5.4	4.7
$\phi_3 \times 10^{-2}$ (m^4)	5.4	4.7
$\phi_4 \times 10^{-2}$ (m^4)	5.4	4.6
$\phi_5 \times 10^{-2}$ (m^4)	5.4	4.5
$\phi_6 \times 10^{-2}$ (m^4)	3.4	3.7
$\phi_7 \times 10^{-2}$ (m^4)	3.4	3.5
$\phi_8 \times 10^{-2}$ (m^4)	3.4	3.0
$\phi_9 \times 10^{-2}$ (m^4)	3.4	2.1
$\phi_{10} \times 10^{-2}$ (m^4)	3.4	1.5

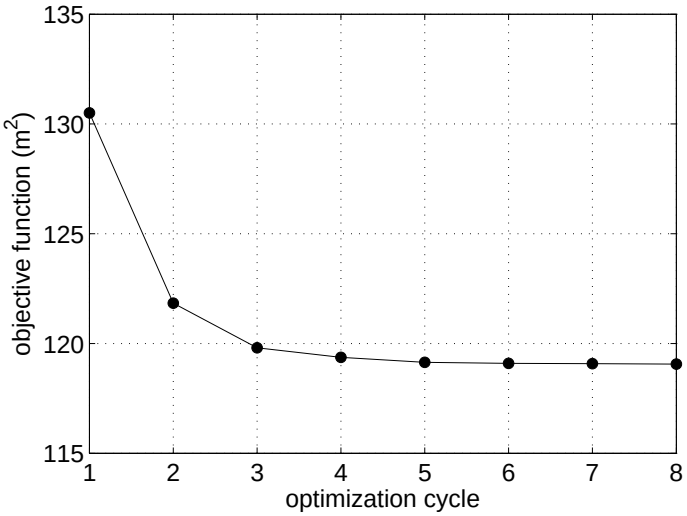

FIG. 5: Iteration history in terms of the objective function.

to acceptable feasible designs better than the initial feasible estimate. This is particularly attractive for dealing with involved problems such as robust stochastic design of base-isolated systems under stochastic excitation.

The effect of the base-isolation system can be observed, for example, from a constraint violation viewpoint. To this end, the failure probability associated with the final design is computed for the case where no base-isolation system is considered. The resulting probability of occurrence of the failure events exceeds the target failure probability ($P_F^* = 10^{-3}$) in more than two orders of magnitude. This result highlights the beneficial effect of the base-isolation system in protecting the superstructure (in this case the 10-story RC frame). The maximum force mobilized in the isolation bearings at the final design is of the order of 25 ton with a maximum base displacement of about 5.0 cm. These values are within the operational range of the devices and, therefore, the final design is physically feasible in terms of the forces and displacements in the lead rubber bearings. The favorable effect of the base-isolation system also can be illustrated by comparing the objective function of the final designs obtained with and without the isolation system. It turns out that the value of the objective function increases about 40% for the final design of the model without the isolation system. Thus, the structural components (columns) at the final design of the model without the isolation system are bigger than the corresponding components of the protected system, as expected. Based on the previous results, the beneficial effect of the base-isolation system is evident.

8.4 Numerical Efforts

The main numerical efforts involved in the solution of the stochastic optimization problem are due to the estimation of the reliability (by means of subset simulation) and its sensitivity. Table 3 summarizes these numerical efforts. The first column in Table 3 indicates the type of analysis performed, while the second column shows the number of times the aforementioned analysis was repeated throughout the optimization procedure. Finally, the third column indicates the average number of simulations required for performing one particular type of analysis. For example, a total of 30 reliability analyses are required for solving the stochastic optimization problem. Each of these analyses involves (on the average) 3000 simulations. Similarly, a total of 30 estimates of the gradient of the probabilities are required for solving the problem, and each of these analyses requires (on the average) 1000 simulations for calibrating the approximate model shown in Eq. (35). The last row of Table 3 indicates the amount of CPU time required to solve the problem in a workstation with an Intel Core 2 Quad processor. This computational cost is substantially different for the case of direct optimization. In that case the number of excursion probability and sensitivity estimations increases dramatically with respect to the proposed approach. In direct optimization the excursion probabilities and their sensitivities need to be estimated for every change of the design variables during the optimization process.

9. CONCLUSION

A general framework for robust reliability-based design of base-isolated buildings under uncertain conditions has been presented. The reliability-based design problem is formulated as a stochastic optimization problem with a single objective function subject to multiple reliability constraints. First excursion probabilities that account for the uncertainties in the system parameters are used to characterize the reliability of the system. The high computational cost associated with the solution of the optimization problem is addressed by the use of approximate reliability analyses during portions of the optimization process. This is achieved by implementing a sequential optimization approach based on global conservative, convex, and separable approximations. The proposed approach takes into account the uncertainty in the system model parameters explicitly during the optimization process. Numerical experience has

TABLE 3: Summary of numerical efforts required to solve the optimization problem

Type of analysis	**Number of analysis required for solving the problem**	**Average number of simulations required per single analysis**
Reliability	30	3000
Gradient of probability	30	1000
CPU time (hour)	1.6	

shown that the algorithm converges in a relatively small number of optimization cycles. This, in turn, implies that only a moderate number of reliability estimates has to be performed during the entire design process. In addition, numerical results have shown that the approach generates a sequence of steadily improved feasible designs. That is, the design process has monotonic convergence properties. This property is particularly attractive for dealing with involved problems such as robust reliability-based optimization of dynamical systems under stochastic excitation. In these problems, which are the cases of interest in this work, each iteration of the optimization process is associated with high computational costs. The results obtained in this work and additional validation calculations highlight the beneficial effects of base-isolation systems in reducing the superstructure response provided that the uncertainty in the system parameters is considered explicitly during the design process. This, in turn, implies more robust and safer designs. Future research directions will aim at expanding the study reported here by considering a sensitivity analysis for model parameters. This type of information gives valuable insight into the effects of uncertain model parameters on the general performance of base-isolated systems.

ACKNOWLEDGMENTS

The research reported here was supported in part by CONICYT under grant number 1110061 which is gratefully acknowledged by the authors.

REFERENCES

1. Ceccoli, C., Mazzotti, C., and Savoia, M., Non-linear seismic analysis of base-isolated rc frame structures, *Earthquake Eng. Struct. Dyn.*, 28(6):633–653, 1999.
2. Chopra, A. K., *Dynamics of Structures: Theory and Applications to Earthquake Engineering*, Prentice Hall, Englewood Cliffs, NJ, 1995.
3. Kelly, J. M., Aseismic base isolation: Review and bibliography, *Soil Dyn. Earthquake Eng.*, 5(4):202–216, 1986.
4. Zou, X.-K., Wang, Q., Li, G., and Chan, C.-M., Integrated reliability-based seismic drift design optimization of base-isolated concrete buildings, *J. Struct. Eng.*, 136(10):1282–1295, 2010.
5. De Luca, A., Mele, E., Molina, J., Verzeletti, G., and Pinto, A. V., Base isolation for retrofitting historic buildings: Evaluation of seismic performance through experimental investigation, *Earthquake Eng. Struct. Dyn.*, 30(8):1125–1145, 2001.
6. Mokha, A. S., Amin, N., Constantinou, M. C., and Zayas, V., Seismic isolation retrofit of large historic building, *J. Struct. Eng.*, 122(3):298–308, 1996.
7. Boore, D. M., Simulation of ground motion using the stochastic method, *Pure Appl. Geophys.*, 160(3-4):635–676, 2003.
8. Baber, T. T. and Y. Wen, Y., Random vibration hysteretic, degrading systems, *J. Eng. Mech. Div.*, 107(6):1069–1087, 1981.
9. Au, S. K. and Beck, J. L., Estimation of small failure probabilities in high dimensions by subset simulation, *Probab. Eng. Mech.*, 16(4):263–277, 2001.
10. Fleury, C. and V. Braibant, V., Structural optimization: A new dual method using mixed variables, *Int. J. Numer. Methods Eng.*, 23(3):409–428, 1986.
11. Groenwold, A. A., Wood, D. W., Etman, L. F. P., and Tosserams, S., Globally convergent optimization algorithm using conservative convex separable diagonal quadratic approximations, *AIAA J.*, 47(11):2649–2657, 2009.
12. Jensen, H. A. and Sepulveda, J. G., Structural optimization of uncertain dynamical systems considering mixed-design variables, *Probab. Eng. Mech.*, 26(2):269–280, 2011.
13. Ditlevsen, O. and Madsen, H. O., *Structural Reliability Methods*, Wiley, New York, 1996.
14. Freudenthal, A. M., Safety and the probability of structural failure, *ASCE Trans.*, 121:1337–1397, 1956.
15. Der Kiureghian, A., Analysis of structural reliability under parameter uncertainties, *Probab. Eng. Mech.*, 23(4):351–358, 2008.
16. Taflanidis, A. A. and Beck, J. L., Stochastic subset optimization for optimal reliability problems, *Probab. Eng. Mech.*, 23(2-3):324–338, 2008.
17. Atkinson, G. M. and W. Silva, W., Stochastic modeling of California ground motions, *Bull. Seismol. Soc. Am.*, 90(2):255–274, 2000.

18. Mavroeidis, G. P. and Papageorgiou, A. S., A mathematical representation of near-fault ground motions, *Bull. Seismol. Soc. Am.*, 93(3):1099–1131, 2003.
19. Kramer, S. L., *Geotechnical Earthquake Engineering*, Prentice Hall, Upper Saddle River, NJ, 2003.
20. Saragoni, G. R. and Hart, G. C., Simulation of artificial earthquakes, *Earthquake Eng. Struct. Dyn.*, 2(3):249–267, 1974.
21. Anderson, J. G. and Hough, S. E., A model for the shape of the Fourier amplitude spectrum of acceleration at high frequencies, *Bull. Seismol. Soc. Am.*, 74(5):1969–1993, 1984.
22. Boore, D. M., Joyner, W. B., and Fumal, T. E., Equations for estimating horizontal response spectra and peak acceleration from western north american earthquakes: A summary of recent work, *Seismol. Res. Lett.*, 68(1):128–153, 1997.
23. Jensen, H. A., Structural optimization of non-linear systems under stochastic excitation, *Probab. Eng. Mech.*, 21(4):397–409, 2006.
24. Prasad, B., Approximation, adaptation and automation concepts for large scale structural optimization, *Eng. Optim.*, 6(3):129–140, 1983.
25. Groenwold, A. A., Etman, L .F. P., Snyman, J. A., and Rooda, J. E., Incomplete series expansion for function approximation, *Struct. Multidiscip. Optim.*, 34(1):21–40,
26. Svanberg, K., A class of globally convergent optimization methods based on conservative convex separable approximations, *SIAM J. Optim.*, 12(2):555–573, 2002. 2007.
27. Chickermane, H. and Gea, H. c., Structural optimization using a new local approximation method, *Int. J. Numer. Methods Eng.*, 39:829–846, 1996.
28. Alexandrov, N. M., Dennis Jr., J. E., Lewis, R. M., and Torczon, V. V., A trust-region framework for managing the use of approximation models in optimization, *Struct. Optim.*, 15(1):16–23, 1998.
29. Haftka, R. T. and Gürdal, Z., *Elements of Structural Optimization*, 3rd ed., Kluwer, Dordrecht, The Netherlands, 1992.
30. Jensen, H. A., Valdebenito, M. A., Schuëller, G. I., and Kusanovic, D. S., Reliability-based optimization of stochastic systems using line search, *Comput. Methods Appl. Mech. Eng.*, 198(49-52):3915–3924, 2009.
31. Ruszczynski, A. and Shapiro, A., *Stochastic Programming*, New York, Elsevier, 2003.
32. Royset, J. O. and E. Polak, E., Reliability based optimal design using sample average approximations, *Probab. Eng. Mech.*, 19:331–343, 2004.
33. Metropolis, N., Rosenbluth, A. W., Rosenbluth, M. N., and Teller, A. H., Equations of state calculations by fast computing machines, *J. Chem. Phys.*, 21(6):1087–1092, 1953.
34. Valdebenito, M. A. and Schuëller, G. I., Efficient strategies for reliability-based optimization involving non linear, dynamical structures, *Comput. Struct.*, 89(19-20): 17971–1811, 2011.